Available online at www.sciencedirect.com

ScienceDirect

IFAC PapersOnLine 50-1 (2017) 12797–12802

A comparison of data-driven fault detection methods with application to aerospace electro-mechanical actuators

M. Mazzoleni *, **Y. Maccarana** *, **F. Previdi** *

* *Department of Management, Information and Production engineering University of Bergamo, via Galvani 2, 24044 Dalmine (BG), Italy (e-mail: mirko.mazzoleni@unibg.it).*

Abstract: In this paper, a model-free framework is proposed in order to equip electro-mechanical actuators, deployed in aerospace applications, with health-monitoring capabilities. A large experimental activity has been carried out to perform acquisitions with both healthy and faulty components, taking into consideration the standard regulations for environmental testing of avionics hardware. The injected faults followed a Fault Tree Analysis and Failure Mode and Effect Analysis. Features, belonging to different domains, have been extracted from the measured signals. These indexes are based largely on the motor driving currents, in order to avoid the installation of new sensors. Finally, a Gradient Tree Boosting algorithm has been chosen to detect the system status: the choice has been dictated by a comparison with other known classification algorithms. Furthermore, the most promising features for a classification point of view are reported.

Keywords: Fault Detection, Machine Learning, Electro-Mechanical Actuators

1. INTRODUCTION

The development of a More Electrical Aircraft (MEA) is a technological transition applied for almost all the systems in aircrafts and helicopters. In such context, the implementation of Electro-Mechanical Actuators (EMAs) has increased rapidly during the last years, as noticed in Isturiz et al. (2010). Mechanical systems deployed in aerospace environments require constraints on weigth and robustness. When no hardware redundancy can be afforded, for safety reasons, an actuator must be equipped with a sophisticated diagnostic, prognostic, and recovery system. The monitoring of mechanical components for Fault Detection and Isolation (FDI) purposes is nowadays well known in literature, as summarized in Capolino et al. (2015). Fault detection and diagnosis systems implement the following tasks, as proposed in Gertler (1998):

- Fault detection: the indication that something deviates from nominal system behaviour
- Fault isolation: the determination of the fault location
- Fault identification: the quantification of the fault magnitude

The isolation and identification tasks together are referred to as fault diagnosis. Fault detection and diagnosis methods are usually classified into model-based and model-free ones, see Venkatasubramanian et al. (2003) and successive works for comprehensive reviews. Regarding the recent employment of data-driven methods in the context of electrical motors, in Choi et al. (2015) a robust diagnosis technique is presented by iteratively analyzing the pattern of multiple fault signatures in a motor current signal. Similarly, Giantomassi et al. (2015) adopt kernel density estimation to evaluate the probability density function of each healthy motor and motor stator fault. A recently proposed model-based FDI application can instead be found in Duan and Živanović (2015), which leverages on parameter estimation for induction motors interturn short circuits detection. Specific works applied on EMAs in the avionics world can be found in Narasimhan et al. (2010) for a combination of model-based and model-free approaches, and in Byington et al. (2004) for model-based philosophy. The former paper tested various types of mechanical (spalling on raceway, actuator jam) and sensors faults, using a compact test bed which can be mounted on an aircraft. Then, data can be acquired during real flights. Tests performed during this project are based on a 1:1 scale actuator. In the latter work, authors focused on simulating failures on transmission gears and bearings.

The work presented in this paper deals instead with ballscrew faults. This work has been carried out under the HOLMES project (Health OnLine Monitoring of Electro-mechanics actuator Safety). The purpose is to develop a health monitoring system to detect mechanical faults for EMAs in aerospace environment. This type of actuators can be used to handle primary and secondary aerodynamic surfaces. The presented material focuses on a specific type of fault, and its presence and degree of severity have to be assessed.

As a *first contribution*, this paper presents the description of an experimental health monitoring project on electro-mechanical actuators for airliner applications. As a *second contribution*, the development of a model-free health monitoring technique to perform fault detection and identification in the previous setting is described. A preliminar

2405-8963 © 2017, IFAC (International Federation of Automatic Control) Hosting by Elsevier Ltd. All rights reserved.
Peer review under responsibility of International Federation of Automatic Control.
10.1016/j.ifacol.2017.08.1837

work by the same authors can be found in Mazzoleni et al. (2014). The methodology is based on a machine learning pipeline, on the assumption that data collected from different system conditions belong to different “classes” that the algorithm learns to discern. This assumption came from the fact that non-ideal mechanical behaviours can be detected by inspecting suitable measurements, such as motor phase currents, see Henao et al. (2014). The chosen algorithm indeed is able to perform correct classifications on the test dataset, which are way better than random assignments. A comparison of different classification algorithms is presented, and the chosen one is a Gradient Tree Boosting classifier. Methods and results are validated by means of experimental tests, via a test rig equipped with a motor and a production-level ballscrew transmission.

The remainder of the paper is organized as follows: in Section 2, the experimental setup is presented and a description of the performed tests is given, along with the collected measurements. In Section 3, the steps involving the design of a model-free fault detection algorithm are outlined. Section 4 shows a comparison between different classifiers, with indications about the choices made, and a graphical visualization of the most important features for fault detection is given. Section 5 is devoted to concluding remarks and future developments.

2. EXPERIMENTAL SETUP

2.1 Application context

As depicted in Fig. 1, the test rig is composed by the main EMA under test, equipped with a ballscrew transmission.

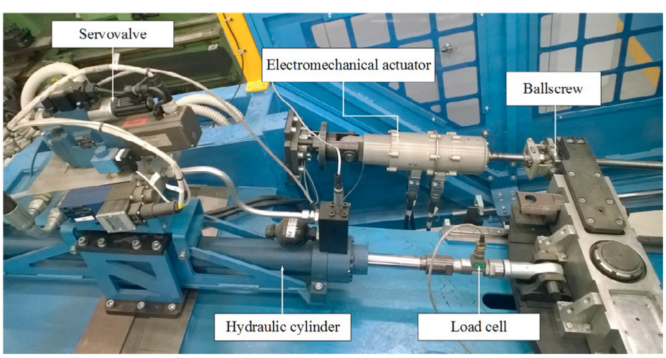

Fig. 1. Test rig with main components. The load cell is used to close the hydraulic cylinder force loop, controlled by the servovalve

The motor consists of a five phases brushless DC motor, which is able to operate even when two phases are open. A nut containing the recirculating spheres moves axially over the screw, transforming the rotation into a linear movement. A hydraulic cylinder, modeled in Cologni et al. (2016), is used to generate the force which the EMA has to overcome during its motion. A load cell is used to close the force control loop. The nut under test has two recirculating circuits, with 80 balls per channel which alternates between steel and ceramic ones, see Fig. 2. The fault investigated in this work consists of the damage undergone by the the steel spheres, at different damage levels. This fault was chosen for investigation after a Fault Tree Analysis (FTA) and a Failure Mode and Effect

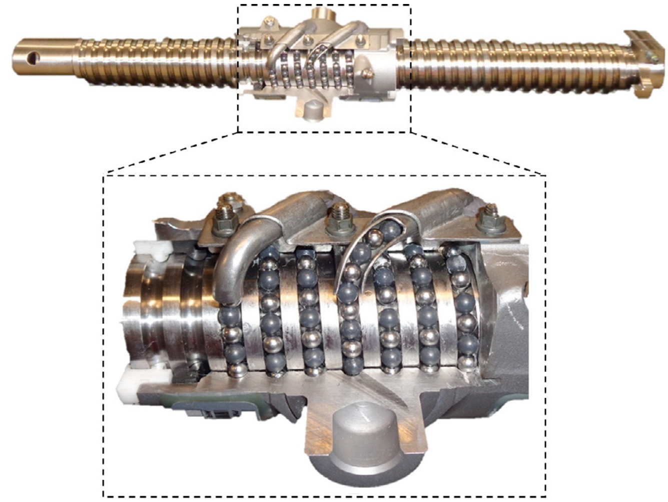

Fig. 2. Ballscrew transmission and recirculation nut detail. The balls alternates between ceramic and steel ones

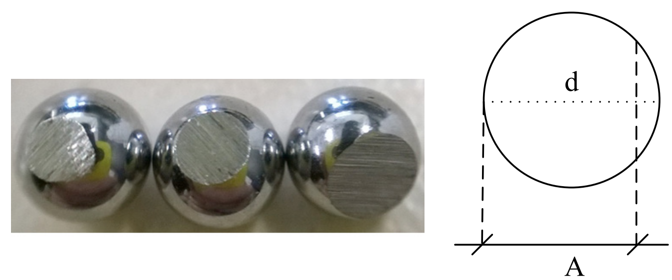

(a) Balls damage detail inside the transmission. From left to rigth: light, medium and high damaged balls

(b) Quantification of ballscrew steel balls injected damages

Fig. 3. Injected faults on ballscrew spheres: qualitative and quantitative views

Analysis (FMEA). The RTCA/DO-160 “Environmental Conditions and Test Procedures for Airborne Equipment” standard has been consulted, and low temperature tests were performed. Other test conditions specified in the standard have not been taken into consideration, because the actuator was proved to be robust to them, or because they were impossible to test.

2.2 Fault implementation and test conditions

As described in Section 2.1, the considered mechanical fault conditions regard the spalling of steel balls inside the ballscrew recirculation nut. The fault was injected by a Electrical Discharge Machine (EDM). This type of fault has been deemed representative of a real one by the ballscrew producer. Three types of damage harshness have been chosen. The fault quantification can be assessed by referring to Fig. 3: the diameter d for healthy balls is 3.5 mm, while, for defected balls, the entity of the fault is respectively:

- Light damage: $A = 3.3\,\mathrm{mm}$
- Medium damage: $A = 3.2\,\mathrm{mm}$
- High damage: $A = 3.1\,\mathrm{mm}$

With the aforementioned damage levels, three fault conditions have been investigated during the test campaigns:

(1) **Fault condition 1**: 6 light damaged + 6 medium damaged + 6 high damaged balls per channel
(2) **Fault condition 2**: 20 high damaged balls per channel
(3) **Fault condition 3**: 40 high damaged balls per channel

These conditions have been chosen in order to enhance the fault condition, by increasing both the number of damaged balls and their damage level. Tests were performed with both healthy and faulty nuts, by simply replacing one nut with another. During acquisition sessions, the temperature was controlled by cooling the actuator after each movimentation to its starting temperature, in order to minimize the uprising of temperature-dependent effects. A number of tests have been also performed by letting the motor temperature to raise up, to study the possible effects of heating on actuator performance. The test campaign's prospect included low temperature tests, which were performed by means of a cold chamber, connected to the metal cage which embedded the actuator, see Fig. 4. This setup allowed to reach temperatures of $-40\,^{\circ}$C via liquid nitrogen injection.

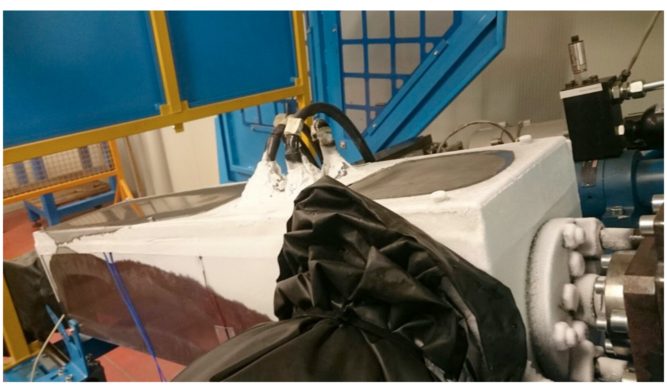

Fig. 4. Low temperature tests setup with motor cage detail

2.3 Test profiles

The whole test bench is controlled via a specific PC bench, which permits to select the desired profiles to be executed. The computer is connected to the electric drive through a Serial Peripheral Interface (SPI) connection, and communicates with the hydraulic cylinder via a National Instrument (NI) CompactRIO hardware. The drive deals with the control of the electric motor speed and current loop, while the CompactRIO computes the control law of the hydraulic piston. The position, or speed, profile is sent via the RS232 protocol to an ECU linked to the motor drive, and has the duty to close the position control loop. The profiles used in the experimentation were discussed with the project partners. The nominal load profile used during the tests corresponds to a typical high lift load profile; additional load profiles with constant 12 kN and 15 kN where employed as shown in Fig. 5, to better assess the fault conditions. Slightly different behaviours in the load response are due to test bench non-idealities. The position profile has been defined as follows:

(1) Position run from 0 mm to 411 mm (100% of the actuator stroke), in 20 s
(2) Acceleration of 2 s, from 0 $\frac{\text{mm}}{\text{s}}$ to 21 $\frac{\text{mm}}{\text{s}}$

In order to cope with the second constraint, the motion profile has been implemented as a speed profile, as depicted in Fig. 6. The experimental tests consisted each in two runs of the aforementioned speed profiles: data are recorded during all runs, but only measurements from the second run are retained for successive processing. This is due to the fact that, during the first motion, test rig's settlements and vibration due to motion starting compromise the validity of acquired data.

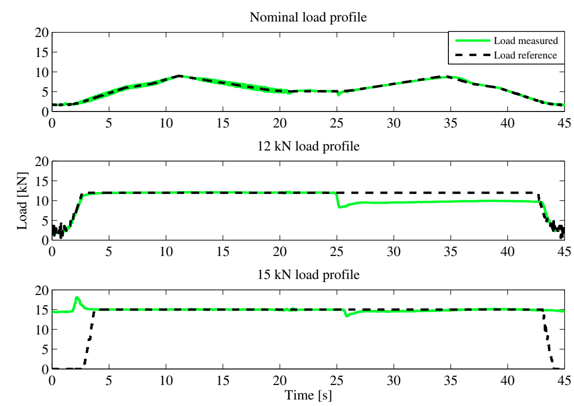

Fig. 5. Load profiles employed during the test sessions. The non-ideal tracking behaviour is due to test bench limitations

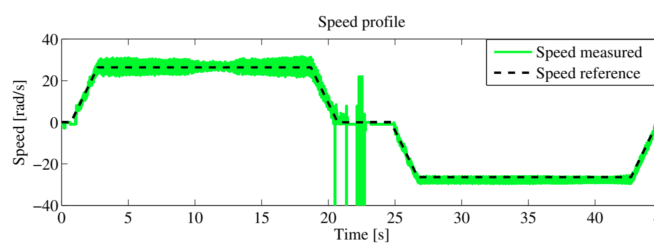

Fig. 6. Speed profile, in radiants/seconds, employed during the test sessions. Spikes and oscillating behaviours are visible

2.4 Measurements

Various measurements have been collected from the test rig's equipped electronic, with the addition of a NI cDAQ device. The modules installed on the cDAQ consisted in a 16 bit voltage module (to acquire the load cell for synchronzation purposes) and current one (to acquire cylinder pressures), along with a 24 bit module used to measure the signals of two piezoelectric accelerometers mounted in orthogonal directions on the nut. The acquisition frequency for the cDAQ was set to 20 kHz; already acquired variables (see Fig. 7), related to the EMA, were acquired at 5 kHz and sent to the PC bench via SPI, while variables related to the hydraulic part were measured at 1 kHz and stored via a NI 6323 16 bit acquisition board. A type K thermocouple was mounted on the motor surface were the magnets lie, and acquired through a Hydra Fluke device. An overall representation of the measurements' information flow is presented in Fig. 7.

Variables used for control Variables that were stored but not used to perform any health monitoring function

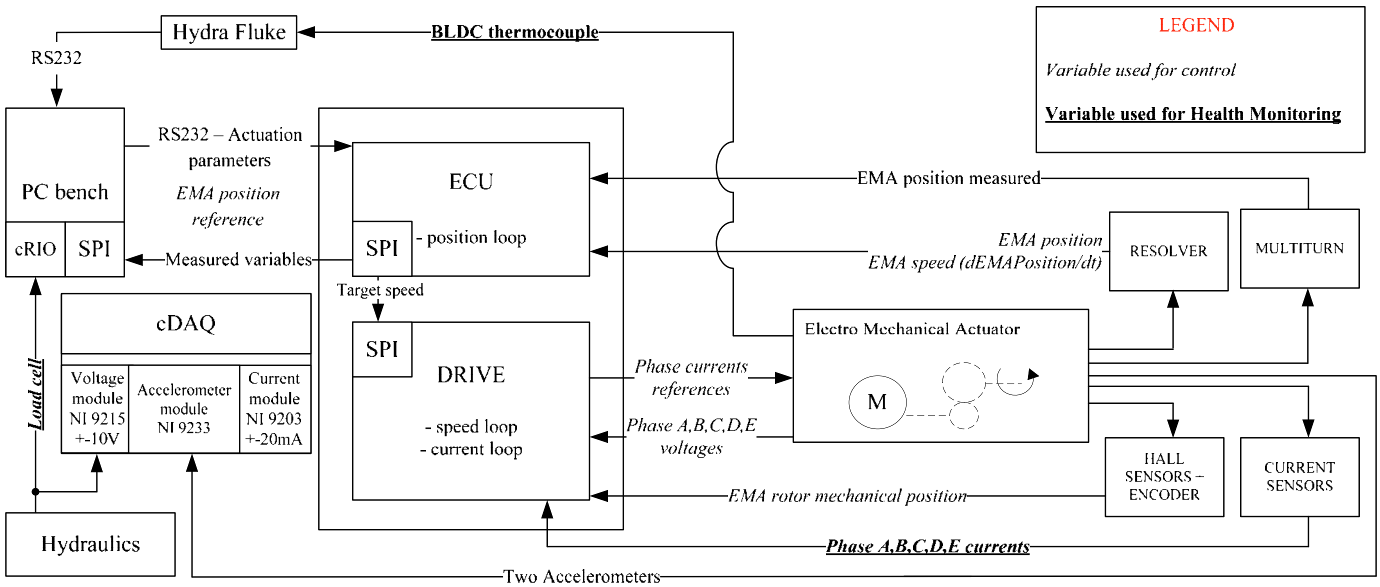

Fig. 7. Schematic of the test rig components, with interactions and measurements system information

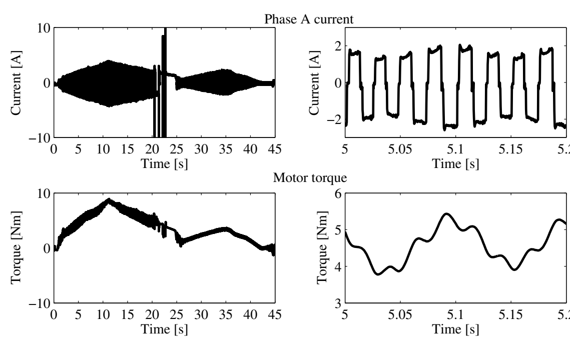

Fig. 8. Top: motor phase A current with detail on current shapes. Bottom: computed motor torque with detail

consist of the motor phase voltage references collected by the motor drive, the motor angular position via a combination of resolver and multiturn encoder measurement, and the motor speed obtained by deriving the position measurement. Variables such as the speed profile were not considered since, being the system in closed loop, a possible fault would be hidden in the speed or position measurements.

Variables used for health monitoring The variables used for the development of the model-free fault detection algorithms are mainly related to phase current measurements, with a current sensor directly installed on the motor drive. The motor's torque, along with the quadrature current, has been computed from the phase currents and the motor mechanical sectors, Fig. 8. The motor's commutation logic is provided by means of hall sensors and an incremental encoder. The motor's torque constant was obtained through bench characterization. Other variables used to compute the fault detection indexes are the load cell and the thermocouple.

3. MODEL-FREE FAULT DETECTION STRATEGY

This section presents the logical steps adopted in order to develop the machine learning based model-free solution. The process pipeline is sketched in Fig. 9, where details about each phase are described. The steps consists into feature extraction, feature selection with classifier design, and classifier evaluation. The motivations behind

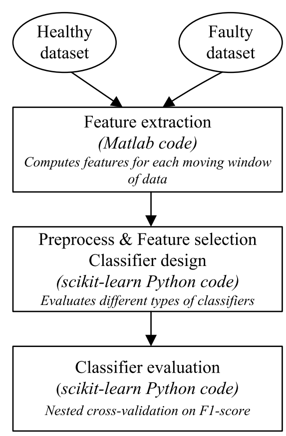

Fig. 9. Model-free methodology flowchart

the data-driven solution over the model-based one has to be sought into complications that arose with the experimental setup at hand. These problematics are related to unknown disturbances and friction characteristics, observed during data analysis, that depend on load entity and position, causing a poor system repeatability. On the other hand, the possibility to perform many experimental tests with different fault conditions, laid the foundation for a model-free approach, which is independent of any modeling, taking a higher vision on the system at hand. The proposed methodology consists in computing features on data obtained through a sliding window, which runs on the entire measurement vectors, selecting each time a portion of data. The length of the sliding window has been chosen, after a sensitivity analysis and guided by a trade-off between computational time and quantity of data on which to compute the features, to be of 1.5 s, with an overlapping factor of 0.75 s. These hyperparameters have to be tuned for the application at hand. Preprocessing of data consisted in filtering noisy signals. The features that are extracted for each data window are described next.

3.1 Feature Extraction

In this work, up to 15 features were computed, spanning time and frequency domain. The indexes are:

(1) Torque-load ratio
(2) Root Mean Square value
(3) Kurtosis
(4) Skewness
(5) Frequency power via FFT transform
(6) Peak-to-valley
(7) Energy operator
(8) Crest factor
(9) Shape factor
(10) Mean frequency
(11) Frequency center
(12) Root Mean Square frequency
(13) Standard deviation frequency
(14) Sixth central moment
(15) Mean temperature

The use and computation of these indexes has been advocated in many previous fault detection applications (see for details the work done by Lei et al. (2010), Benbouzid (2000), Combastel et al. (2002), Rauber et al. (2010), Zarei (2012)). Feature 1 is computed by taking the ratio of the computed motor torque over the load measured by load cell mounted on the hydraulic cylinder. Features from 2 to 14 are computed on the motor quadrature current signal, while feature 15 is computed from the thermocouple measurements. The considered spectrum in Feature 6 is $(0\,\mathrm{Hz} - 50\,\mathrm{Hz}]$, since the major frequency content of the quadrature current lies in that range. Then, the total frequency power in that range is used as feature. The output of this stage is a feature matrix X. This choice of measurements has been demanded by the application: the aim was indeed to rely mainly on electrical variables to perform the health monitoring.

3.2 Feature Selection and classifier design

The data were then divided into train (80%) and test (20%) set. The train data were then scaled via a robust standardization procedure (Rousseeuw and Croux (1992)), which, for each feature, removes the median and divides for the interquantile range (the interval between the 25th quantile and the 75th quantile). This standardization was chosen because it is more robust to outliers in the data. The transformation, with parameters fitted on the training set, is then applied to the test set. Then, various types of classification algorithms were tested, such as: Logistic Regression (LR), Support Vector Machine (SVM), Naïve Bayes (NB) and Gradient Tree Boosting (GTB) (see Friedman et al. (2001) for details). All chosen classifiers are discriminative, except for the Naïve Bayes one. The choice is dictated by the fact that the classification result is of most interest with respect to understand the data-generating process. However, it is useful to test both classifier types, given that, under certain conditions, generative classifiers can reach faster their maximum accuracy bound with respect to discriminative algorithms, see Jordan (2002). The hyperparameters of each algorithm have been found by using a 5-fold cross-validation (cv) on the train set. The selected model is then trained on the training data. The logistic regression classifier was equipped with a $L2-$regularization term, and the relative hyperparameter was tuned. The Support Vector Machine classifier used a Radial Basis Function kernels which required to find the proper parameters value. Regarding the Naïve Bayes algorithm, the Gaussian likelihood was assumed. Tune parameters of the Gradient Tree Boosting method were the number of tree estimators, the subsample percentage and the learning rate.

3.3 Classifier evaluation

The evaluation of each classifier is done through two different procedures. As a first performance check, the classifiers were evaluated on the test set, and the mean F1-score (Powers, 2011) is reported. A value of 1 indicates perfect classification, while a value of 0 indicates a completely wrong result. Since the F1-score is defined for a binary classification problem, we end up with four F1-scores, since in this formulation there are four classes into which classify the data (Healthy, Fault 1, Fault 2, Fault 3). This score is computed by taking the weighted mean of the four F1-scores. The weights are the percentage of observations for a specific class over the total number of tests points. This choice of metric is due to the fact that it better assesses cases of imbalanced classes as opposed to classification accuracy.

To check the stability of the training procedure, including also the steps performed to find the best hyperparameters, a nested cross-validation can be employed. It has been shown in Cawley and Talbot (2010) that this method better assesses the true algorithm performance, giving a less biased estimation with respect to the stardard cross-validation with fixed parameters, which would lead to an optimistic evaluation. With this method, each train/test fold may get different hyperparameter settings, resulting in an algorithm that internally finds the best parameters for each data set it gets. The results of this procedure are then reported as estimation of the model true performance. In this work a 5-fold nested-cv has been used on all the data (training + test dataset). As before, the weighted F1-score has been applied as performance metric. The feature scaling is fit on the training fold and applied on the test ones, for each training/testing folds combinations. The output is a vector of 5 weighted F1-scores, and the mean and standard deviation of this vector is taken as performance metric for classifiers comparison. This leads to an estimation of the mean F1-score with associated standard error. If the standard error is high, it means that the found hyperparameters are not reliable, and the learned model, with hyperparameters selected via cross-validation on the training set (or on all available data) can not be deployed into production.

Table 1. Classifiers comparison summary

Classifier	Mean Test set F1-score	Mean Nested cv F1-score	Std. error Nested cv F1-score
LR	0.25	0.21	0.024
SVM	0.70	0.70	0.005
NB	0.13	0.12	0.006
GTB	0.83	**0.82**	0.009

4. RESULTS DISCUSSION

The final comparison results are reported in Table 1. The best performing classifier is the Gradient Tree Boosting algorithm, with a weigted mean F1-score obtained through nested cross-validation of 0.82. The Logistic Regression adn Naïve Bayes algorithm failed to properly capture most of the data traits, not being enough flexible in their decision boundaries. The low standard error of the mean F1-score obtained by nested cross-validation indicates that the procedure used to select the classifiers hyperparameters is stable, not exibiting large variations when different datasets are used to tune them. Fig. 10 depicts the importance of each feature used, as considered by the GTB algorithm. The most informative indexes, as concerns the classification point of view, are the cage temperature, the torque to load ratio, and the computed frequency content.

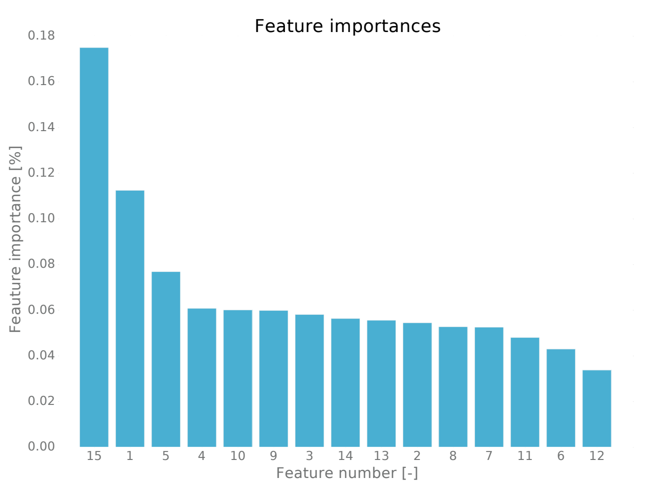

Fig. 10. Features importance

5. CONCLUSIONS AND FUTURE DEVELOPMENTS

This paper presented a practical approach to the fault detection and identification problem. The application described regarded the health monitoring of mechanical components for electro-mechanical actuators deployed in an aerospace environment. Future developments include the combination of the proposed approach with a model-based methodology, and applications of the framework to other fault types and conditions.

ACKNOWLEDGEMENTS

This research activity has been carried out in the context of the research project *HOLMES* funded by CleanSky Joint Technology Initiative, funding scheme FP7-JTI-CS and Grant Agreement number 338549.

REFERENCES

Benbouzid, M.E.H. (2000). A review of induction motors signature analysis as a medium for faults detection. *IEEE transactions on industrial electronics*, 47(5), 984–993.

Byington, C.S., Watson, M., Edwards, D., and Stoelting, P. (2004). A model-based approach to prognostics and health management for flight control actuators. In *Aerospace Conference, 2004. Proceedings. 2004 IEEE*, volume 6, 3551–3562. IEEE.

Capolino, G.A., Antonino-Daviu, J.A., and Riera-Guasp, M. (2015). Modern diagnostics techniques for electrical machines, power electronics, and drives. *IEEE Transactions on Industrial Electronics*, 62(3), 1738–1745.

Cawley, G.C. and Talbot, N.L. (2010). On over-fitting in model selection and subsequent selection bias in performance evaluation. *Journal of Machine Learning Research*, 11(Jul), 2079–2107.

Choi, S., Pazouki, E., Baek, J., and Bahrami, H.R. (2015). Iterative condition monitoring and fault diagnosis scheme of electric motor for harsh industrial application. *IEEE Transactions on Industrial Electronics*, 62(3), 1760–1769.

Cologni, A., Mazzoleni, M., and Previdi, F. (2016). Modeling and identification of an electro-hydraulic actuator. In *2016 12th IEEE International Conference on Control and Automation (ICCA)*, 335–340. IEEE.

Combastel, C., Lesecq, S., Petropol, S., and Gentil, S. (2002). Model-based and wavelet approaches to induction motor on-line fault detection. *Control Engineering Practice*, 10(5), 493–509.

Duan, F. and Živanović, R. (2015). Condition monitoring of an induction motor stator windings via global optimization based on the hyperbolic cross points. *IEEE Transactions on Industrial Electronics*, 62(3), 1826–1834.

Friedman, J., Hastie, T., and Tibshirani, R. (2001). *The elements of statistical learning*, volume 1. Springer series in statistics Springer, Berlin.

Gertler, J. (1998). *Fault Detection and Diagnosis in Engineering Systems*. Electrical Engineering and Electronics. Taylor & Francis.

Giantomassi, A., Ferracuti, F., Iarlori, S., Ippoliti, G., and Longhi, S. (2015). Electric motor fault detection and diagnosis by kernel density estimation and kullback–leibler divergence based on stator current measurements. *IEEE Transactions on Industrial Electronics*, 62(3), 1770–1780.

Henao, H., Capolino, G.A., Fernandez-Cabanas, M., Filippetti, F., Bruzzese, C., Strangas, E., Pusca, R., Estima, J., Riera-Guasp, M., and Hedayati-Kia, S. (2014). Trends in fault diagnosis for electrical machines: A review of diagnostic techniques. *IEEE industrial electronics magazine*, 8(2), 31–42.

Isturiz, A., Vinals, J., Fernandez, S., Basagoiti, R., Torre Arnanz, E.d.l., and Novo, J. (2010). Development of an aeronautical electromechanical actuator with real time health monitoring capability.

Jordan, A. (2002). On discriminative vs. generative classifiers: A comparison of logistic regression and naive bayes. *Advances in neural information processing systems*, 14, 841.

Lei, Y., Zuo, M.J., He, Z., and Zi, Y. (2010). A multidimensional hybrid intelligent method for gear fault diagnosis. *Expert Systems with Applications*, 37(2), 1419–1430.

Mazzoleni, M., Formentin, S., Previdi, F., and Savaresi, S.M. (2014). Fault detection via modified principal direction divisive partitioning and application to aerospace electro-mechanical actuators. In *53rd IEEE Conference on Decision and Control*, 5770–5775. IEEE.

Narasimhan, S., Roychoudhury, I., Balaban, E., and Saxena, A. (2010). Combining model-based and feature-driven diagnosis approaches-a case study on electromechanical actuators.

Powers, D.M. (2011). Evaluation: from precision, recall and f-measure to roc, informedness, markedness and correlation.

Rauber, T.W., do Nascimento, E.M., Wandekokem, E.D., and Varejão, F.M. (2010). *Pattern recognition based fault diagnosis in industrial processes: review and application.* INTECH Open Access Publisher.

Rousseeuw, P.J. and Croux, C. (1992). Explicit scale estimators with high breakdown point. *L1-Statistical analysis and related methods*, 1, 77–92.

Venkatasubramanian, V., Rengaswamy, R., Yin, K., and Kavuri, S.N. (2003). A review of process fault detection and diagnosis: Part i: Quantitative model-based methods. *Computers & chemical engineering*, 27(3), 293–311.

Zarei, J. (2012). Induction motors bearing fault detection using pattern recognition techniques. *Expert systems with Applications*, 39(1), 68–73.